

## ORIGINAL ARTICLE

## Effect of vascular endothelial growth factor gene therapy on post-traumatic peripheral nerve regeneration and denervation-related muscle atrophy

S Moimas<sup>1,2,6</sup>, F Novati<sup>3,6</sup>, G Ronchi<sup>4,5</sup>, S Zacchigna<sup>1</sup>, F Fregnan<sup>4,5</sup>, L Zentilin<sup>1</sup>, G Papa<sup>3</sup>, M Giacca<sup>1,2</sup>, S Geuna<sup>4,5</sup>, I Perroteau<sup>4</sup>, ZM Arnez<sup>3</sup> and S Raimondo<sup>4,5</sup>

Functional recovery after peripheral nerve injury depends on both improvement of nerve regeneration and prevention of denervation-related skeletal muscle atrophy. To reach these goals, in this study we overexpressed vascular endothelial growth factor (VEGF) by means of local gene transfer with adeno-associated virus (AAV). Local gene transfer in the regenerating peripheral nerve was obtained by reconstructing a 1-cm-long rat median nerve defect using a vein segment filled with skeletal muscle fibers that have been previously injected with either AAV2-VEGF or AAV2-LacZ, and the morphofunctional outcome of nerve regeneration was assessed 3 months after surgery. Surprisingly, results showed that overexpression of VEGF in the muscle-vein-combined guide led to a worse nerve regeneration in comparison with AAV-LacZ controls. Local gene transfer in the denervated muscle was obtained by direct injection of either AAV2-VEGF or AAV2-LacZ in the flexor digitorum sublimis muscle after median nerve transection and results showed a significantly lower progression of muscle atrophy in AAV2-VEGF-treated muscles in comparison with muscles treated with AAV2-LacZ. Altogether, our results suggest that local delivery of VEGF by AAV2-VEGF-injected transplanted muscle fibers do not represent a rational approach to promote axonal regeneration along a venous nerve guide. By contrast, AAV2-VEGF direct local injection in denervated skeletal muscle significantly attenuates denervation-related atrophy, thus representing a promising strategy for improving the outcome of post-traumatic neuromuscular recovery after nerve injury and repair.

*Gene Therapy* (2013) 20, 1014–1021; doi:10.1038/gt.2013.26; published online 30 May 2013

**Keywords:** adeno-associated virus; VEGF; peripheral nerve; skeletal muscle; rat

## INTRODUCTION

Gene therapy is an emerging issue in tissue engineering of damaged organs including those belonging to the neuromuscular system.<sup>1,2</sup> One of the potential applications of gene therapy is represented by the treatment of traumatic nerve injuries. In fact, following nerve damage, axon continuity is interrupted and the distal axonal tract goes toward degeneration.<sup>3</sup> As a consequence, the anatomical and functional connections between motoneurons and skeletal muscle fibers are lost inducing a progressive muscle atrophy.<sup>4,5</sup> If nerve continuity is guaranteed (by surgical repair), the proximal stump of damaged axons can regenerate within the distal nerve stump, reach the denervated muscle and restore functional connection with it.<sup>3</sup>

As muscle atrophy is accompanied by a progressive loss-of-function recovery after reinnervation,<sup>6–8</sup> the lapse of time between the traumatic event and the restoration of the neuromuscular function is one of the key factors for the eventual functional recovery. For this reason, improvement of motor function recovery after traumatic nerve injury and repair can be obtained by both accelerating axonal regeneration, thus reducing the denervation time lapse, and decelerating the progression of skeletal muscle atrophy, thus improving its

capacity to restore function when regenerated axons eventually reach it.

Gene therapy based on adeno-associated virus (AAV) appear to be a rational approach to reach this goal as AAVs have already been used to efficiently deliver therapeutic genes to muscle and nerve, and to induce muscle/neural protection and repair in different experimental models.<sup>1,9–13</sup>

Various genes are candidates for promoting peripheral axon regeneration<sup>14</sup> and preventing muscle atrophy, including VEGF.<sup>13,15–19</sup> Haninec *et al.*<sup>16</sup> demonstrated that increasing VEGF protein in nerve stumps resulted in a higher quality of axon regeneration and functional reinnervation after both end-to-end and end-to-side neurorrhaphy. In particular, VEGF was shown to promote axonal outgrowth and Schwann cell proliferation.<sup>16</sup> Moreover, Sondell *et al.*<sup>17</sup> reported that VEGF was able to stimulate Schwann cell invasion and neovascularization after a sciatic nerve transection. Yet, several studies highlighted that VEGF interacts with satellite cells of skeletal muscle and promotes its regeneration after trauma.<sup>13,18,20</sup> Moreover, VEGF was shown to have an antiapoptotic and a direct myogenic effect,<sup>13</sup> and to be able to enhance muscle force restoration and reduced the amount of connective tissue after traumatic injury.<sup>18</sup>

<sup>1</sup>Molecular Medicine Laboratory, International Centre for Genetic Engineering and Biotechnology (ICGEB), Trieste, Italy; <sup>2</sup>Department of Medical Sciences, Faculty of Medicine, University of Trieste, Trieste, Italy; <sup>3</sup>Department of Plastic and Reconstructive Surgery, Cattinara Hospital, University Hospital of Trieste, Trieste, Italy; <sup>4</sup>Department of Clinical and Biological Sciences, University of Turin, Orbassano, Italy and <sup>5</sup>Neuroscience Institute Cavalieri Ottolenghi, Orbassano, Italy. Correspondence: Dr S Raimondo, Department of Clinical and Biological Science, University of Turin, Regione Gonzole 10, 10043 Orbassano, Italy. E-mail stefania.raimondo@unito.it

<sup>6</sup>These authors contributed equally to this work.

Received 21 December 2012; revised 11 April 2013; accepted 24 April 2013; published online 30 May 2013

Therefore, we wondered whether VEGF overexpression may exert a positive effect on both post-traumatic axonal regeneration and denervation-related muscle atrophy in a rat upper limb model.<sup>21</sup>

## RESULTS

### Evaluation of AAV muscle transduction

In Figure 1 results of the pilot study performed to evaluate the efficiency of AAV muscle infection are reported. Viral DNA persistence (Figures 1a and c) and transgene expression (Figures 1b and d) were analyzed in the two models used in this study: (i) peripheral nerve regeneration and (ii) skeletal muscle atrophy.

In the model of peripheral nerve regeneration, AAVs were injected in the pectoralis major muscle 14 days before main surgery in order to allow proper transgene expression. The area of injection was marked by two suture stitches and, to confirm the identification of the transduced muscle for the generation of the muscle-in-vein (MIV) conduit, we assessed both vector persistence and transgene expression in a portion of muscle withdrawn from the area of injection but not used for the conduit. We evaluated also the presence of the viral DNA and the expression of the transgene in the MIV conduit withdrawn 14 days after surgery. Viral genomes were found in the MIV conduit (Figure 1a) and the expression of the transgene was detectable (Figure 1b), even if a decrease was observed for both parameters. The reduction in the number of viral genomes might be explained both by the loss of nonnuclear DNA, as previously reported,<sup>22</sup> or by the lowering in the number of healthy muscle fibers inside the MIV conduit, as described in the following paragraphs. Concerning the reduction in transgene expression, it might be due to the loss of muscle fiber within the conduits, as already mentioned.

In the second experimental model, AAV injection and muscle denervation were performed at the same time. We evaluated the viral persistence as well as the transgene expression at the moment of tissue withdrawal, and we were able to detect the presence of viral DNA as well as the expression of the transgenes in the transduced flexor digitorum sublimis muscles, 14 days after injection. As reported in Figures 1c and d, AAVs were found to persist in the injected muscle and transgene expression was also detected.

### Peripheral nerve regeneration

Functional recovery and stereological analysis results are shown in Figure 2.

Three months after nerve surgery all animals underwent functional assessment by grasping test, and rats belonging to the MIV-VEGF group showed a significant worse functional recovery than MIV-LacZ rats (Figure 2a). Stereological results showed that the MIV-VEGF group had significantly less fibers (Figure 2b) that were significantly bigger than controls (Figure 2c), whereas the myelin thickness was similar in the two groups (Figure 2c).

Morphological observation provided an explanation of the functional and stereological results. Light microscopy (Figures 3a–d) showed that the worse functional recovery and the lower number of fibers in the MIV-VEGF group was justified by the fact that muscle fibers were still abundant in the graft (Figures 3a and b), whereas in control (MIV-LacZ) group less muscle fibers were detected (Figures 3c and d). By electron microscopy analysis, muscle fibers in the graft of MIV-VEGF showed a reduced atrophy (Figures 3e and f) in comparison with control samples (Figures 3g and h). Indeed, in MIV-VEGF group several myotubes, not detected in controls, could be observed inside the graft (Figure 3e). Moreover, sarcomeres were still well organized and mitochondria were still intact (Figure 3f). In MIV-LacZ, muscle fibers were absent

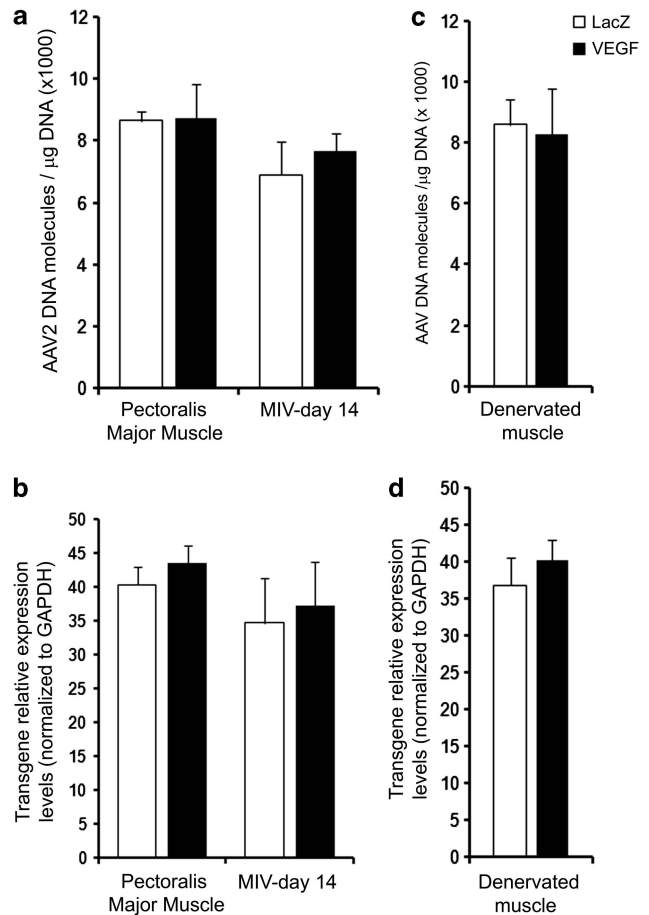


**Figure 1.** Histograms showing viral DNA as well as transgene expression in the injected tissues. Peripheral nerve regeneration model (a and b; number of rats analyzed = 16): quantification of viral DNA in the pectoralis major muscle used to fill the MIV conduit at the moment of surgery and in the MIV conduits 14 days after surgery, quantified by real-time PCR (a); transgene relative expression quantification in the pectoralis major muscle used to fill the MIV conduit at the moment of surgery and in the MIV conduits 14 days after surgery; results are expressed after normalization over the levels of the housekeeping gene *GAPDH* (b). Skeletal muscle atrophy model (c and d; number of rats analyzed = 8): quantification of viral DNA in the flexor digitorum sublimis muscle withdrawn 14 days after denervation and infection, quantified by real-time PCR (c); transgene relative expression quantification in the flexor digitorum sublimis muscle withdrawn 14 days after denervation and infection; results are expressed after normalization over the levels of the housekeeping gene *GAPDH* (d).

(Figures 3c and d) or had evident sign of vacuolization, sarcomeric disorganization and destroyed mitochondria (Figures 3g and h). In MIV-VEGF, there was also a higher number of blood vessels in comparison with MIV-LacZ (data not shown).

Moreover, gene expression analysis of genes involved in the apoptotic process, such as *Bcl2l11*, *Bmf* and *Bad*, showed that in the MIV-VEGF samples the levels of pro-apoptotic genes were reduced, suggesting an antiapoptotic role of VEGF on muscle fibers<sup>13,23</sup> (Supplementary Figure 1).

### Prevention of muscle atrophy

One month after denervation and treatment with AAV2-VEGF, the denervated muscles had a significantly higher weight ( $121 \pm 11$  mg) than muscles treated with AAV2-LacZ ( $96 \pm 5$  mg).

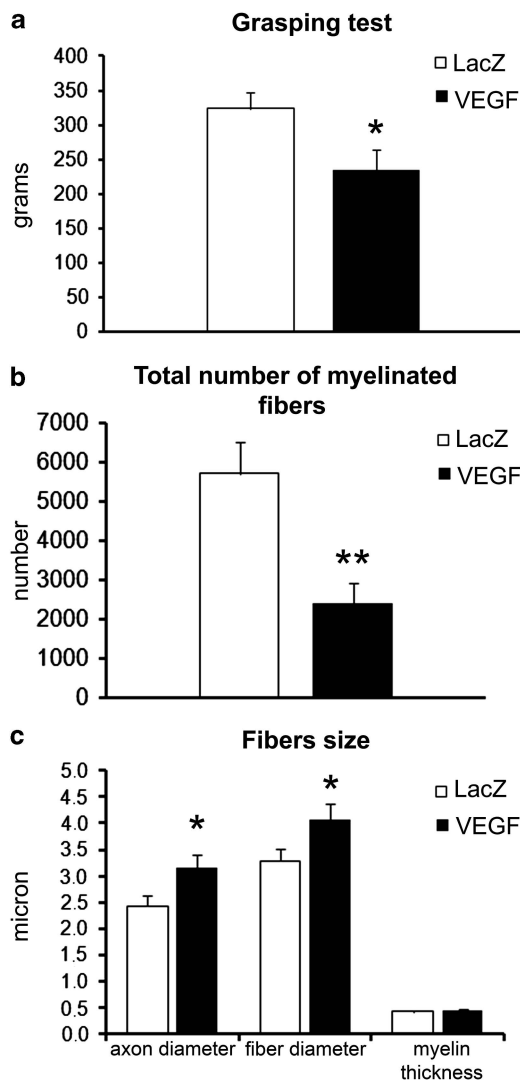


**Figure 2.** Histograms showing the results of functional recovery evaluated by grasping test (a) and the results of morphometrical evaluation of nerve regeneration, (b) number of myelinated fiber in the distal part of the median nerve, (c) axon and fibers diameter and myelin thickness in MIV-LacZ and MIV-VEGF groups (number of rats analyzed = 14). \* $P \leq 0.05$ ; \*\* $P \leq 0.01$ .

Light microscopy on semithin sections stained with toluidine blue of normal muscle (Figure 4a) and denervated muscle 1 month after treatment with AAV2-LacZ (Figure 4b) or AAV2-VEGF (Figure 4c) showed that muscles treated with AAV2-VEGF had a reduced atrophy in comparison with denervated muscles treated with AAV2-LacZ. In fact, muscle fibers treated with AAV2-LacZ were smaller than AAV2-VEGF and had evident signs of sarcomeric disorganization with a greater amount of connective tissue (Figure 4b). The different size of muscle fibers was also confirmed by statistical analysis of stereological data (Figure 4d).

In addition to the observed effect of VEGF on fiber size, we also showed a preferential protective effect of VEGF on skeletal fast fibers. Immunofluorescence analysis of muscle sections showed that VEGF overexpression had almost no effect on slow fiber cross-sectional area, whereas the fast fiber cross-sectional area was significantly increased compared with the denervated muscle treated with AAV-LacZ ( $29\% \pm 5\%$  vs  $44\% \pm 7\%$ , AAV-LacZ and AAV-VEGF, respectively). Representative images and fiber

cross-sectional area quantification are reported in Figures 5a and b, respectively.

## DISCUSSION

Whereas a large body of research has been carried out over the last 20 years for improving post-traumatic peripheral nerve regeneration, the clinical outcome of nerve reconstruction is often still unsatisfactory.<sup>24–26</sup> In a clinical setting of peripheral nerve damage, both nerve and muscles undergo a degeneration process and the identification of molecules able to foster nerve regeneration as well as to protect skeletal muscle from atrophy is thus required. As VEGF is known to promote axonal regeneration and protect muscle fibers from degeneration,<sup>19,27</sup> the present study was aimed at exploring the possibility to effectively use a local gene therapy approach aimed to overexpress VEGF in order to improve functional recovery after peripheral repair.

VEGF is a growth factor that has been used in various animal models of neurodegeneration and the findings are not always clear-cut. The outcome in each study may depend on the variables of that particular study, for example, lesion model, concentration of VEGF used, route-of-delivery and so on. To be successful with VEGF therapy is important to consider all these parameters.

Owing to relatively short (~30–45 min) half-life of VEGF,<sup>28</sup> a carrier is needed to release VEGF in a controlled fashion in order to obtain a sustained effect. Therefore, we used AAV-VEGF gene therapy that is an efficient and stable gene transfer method to bypass this limitation. The features of the AAV life cycle, including its defectiveness and ability to persist in transduced cells as a latent viral episome, suggested early on that this virus appears to be an excellent tool for *in vivo* gene transfer. Over the last few years, AAVs have gained increasing popularity because of the high efficiency of transduction of post-mitotic tissues such as muscle.<sup>9,29,30</sup> The main goals of our study were twofold: to foster axonal regeneration along muscle-vein-combined conduits<sup>31,32</sup> used to bridge a 1-cm-long rat median nerve gap and to prevent denervation-related atrophy of fingers flexor muscle after complete rat median nerve transection.<sup>21</sup> The muscle-vein-combined conduit was chosen in our study to repair injured nerve because of the high efficiency of muscle infection with AAV, and thus it seemed to be a good method for VEGF local delivery.

Results can be summarized as follows: (i) AAV2-VEGF injection succeeded in gene transfer into muscle tissue, (ii) in both experimental models, local VEGF delivery prevented muscle atrophy progression; (iii) whereas muscle atrophy prevention represents a positive prognostic factor for neuromuscular recovery, local VEGF delivery inside the muscle-vein-combined conduit resulted in a significantly reduced functional recovery in comparison with controls.

These observations confirm that skeletal muscle is a good means for AAV-mediated local delivery of secreted molecules,<sup>29</sup> as already shown in preclinical studies and clinical trials for treatment of hemophilia B.<sup>33–35</sup> Indeed, clinical trials have already been concluded and showed good results on restoration of protein levels as reviewed in study by Buning<sup>36</sup> and Giacca.<sup>36,37</sup> Gene therapy with AAVs has been growing in the last years and many serotypes have been identified for the transduction of post-mitotic tissues such as skeletal muscles, hearts, neurons and retina.<sup>38,39</sup> Among the serotype that are reported to be able to transduce skeletal muscles, in previous works from our laboratory,<sup>39</sup> we showed that serotype 2 displays good transduction efficiency when directly injected into the skeletal muscle;<sup>12,13,39–41</sup> indeed, we choose this serotype to study the effect of VEGF overexpression in our animal models of nerve regeneration and muscle atrophy.

In this study, AAVs were injected in the pectoralis major muscle and, to confirm transduction efficiency and transgene expression, we quantified the number of viral genomes and the expression levels both at the moment of muscle withdrawal and 14 days after

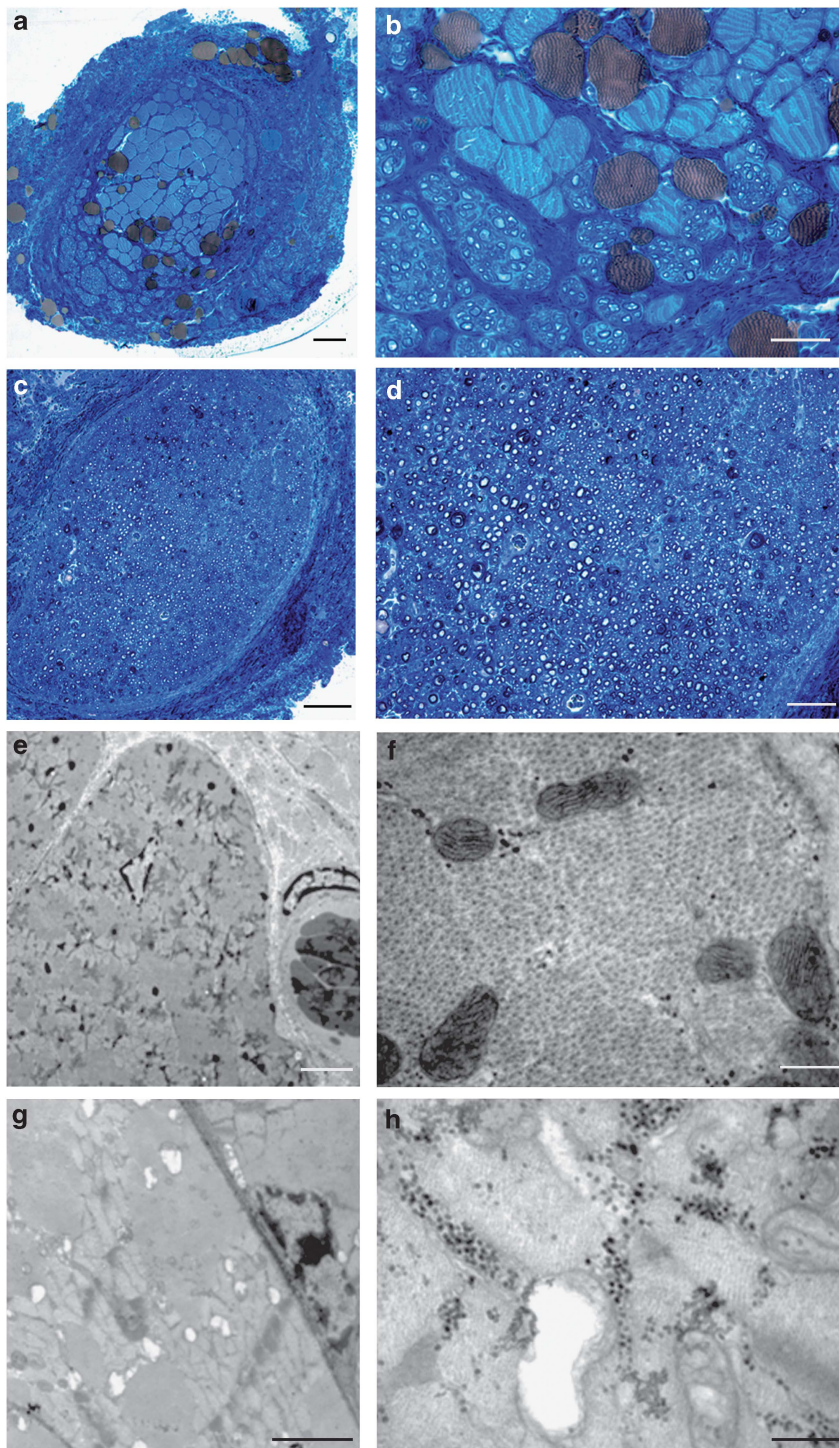


**Figure 3.** Toluidine blue-stained semithin sections observed in light microscopy (**a–d**) and electron microscopy (**e–h**) images of MIV-LacZ (**c, d, g, h**) and MIV-VEGF (**a, b, e, f**) conduits 3 months after surgery. In MIV-VEGF there are a lot of muscle fibers still in the conduit that have well-organized sarcomeres and intact mitochondria. Some myotube with central nucleus are also detectable inside the MIV-VEGF conduit (arrow). In MIV-LacZ conduit the very few muscle fibers that can be observed have different sign of atrophy, such as sarcomeric disorganization, vacuolization and mitochondria destruction. Scale bars: (**a** and **c**): 50  $\mu\text{m}$ ; (**b** and **d**): 20  $\mu\text{m}$ ; (**e** and **g**): 5  $\mu\text{m}$ ; (**f** and **h**): 1  $\mu\text{m}$ .

main surgery. We showed, in agreement with our previous data,<sup>39</sup> that we were able to transduce the muscle and that transgene expression was detectable also within the MIV conduit. The presence of transgene expression was also analyzed by histology and transduced fibers were detected (data not shown).

As far as target muscles are concerned, we observed the occurrence of denervation-related muscle atrophy in both experimental models as expected. We investigated muscle atrophy after 1 month of denervation because it has been shown that this post-denervation time point is sufficient to induce

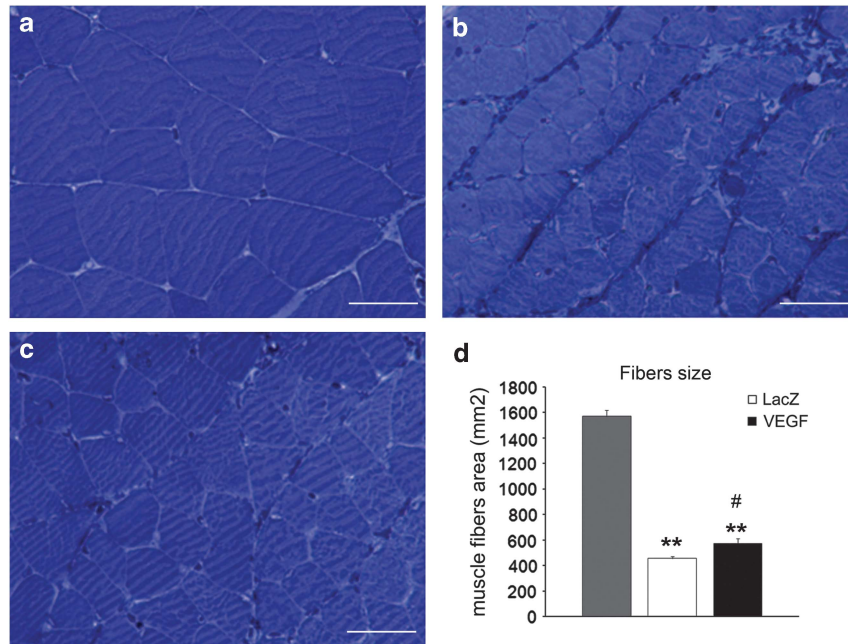


**Figure 4.** Light microscopy of toluidine blue-stained semithin sections of a normal muscle (**a**) and denervated muscle 1 month after surgery and treatment with AAV-LacZ (**b**) or AAV-VEGF (**c**). Histogram in **d** shows the results of morphometrical evaluation of muscle fibers size (number of rats analyzed = 17). # $P \leq 0.05$  VEGF vs LacZ; \*\* $P \leq 0.01$  VEGF and LacZ vs control (CTRL). Scale bars: 25  $\mu$ m.

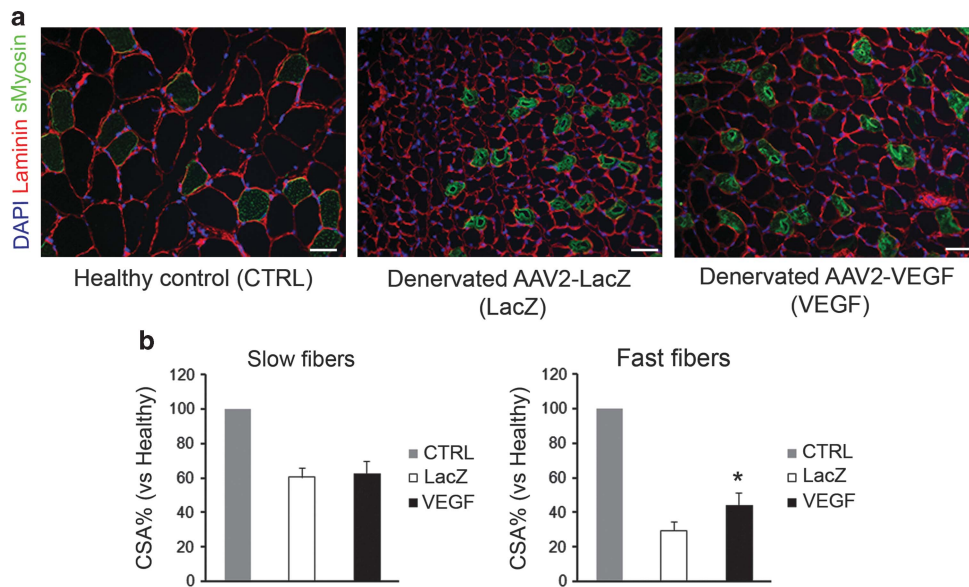


**Figure 5.** Muscle sections were stained in immunohistochemistry with laminin (red) and slow myosin (green) in order to study the effect of VEGF overexpression on skeletal muscle fiber cross-sectional area. Cellular nuclei were counterstained with 4',6-diamidino-2-phenylindole (DAPI; blue). Scale bars: 25  $\mu$ m (**a**). Histograms that represent quantification of the fiber cross-sectional area (**b**); results are expressed as a percentage compared with the matched fiber type in the contralateral healthy muscle (number of rats analyzed = 6). \* $P \leq 0.05$  VEGF vs LacZ.

severe fiber atrophy in rat flexor digitorum sublimis muscle.<sup>42</sup> However, the degree of denervation-related muscle atrophy was significantly lower in AAV-VEGF-treated muscles, suggesting that local delivery of AAV-VEGF in denervated muscle should be seen as a rational strategy for limiting atrophy progression, and thus eventually improving functional recovery after nerve reconstruction.

During skeletal muscle atrophy the ubiquitin-proteasome system is a key player, and a connection among VEGF and the proteasome has already been published.<sup>43,44</sup> Therefore, the VEGF

protective role that we observed might be due to an inhibition of the ubiquitin-proteasome. Another possible explanation relies on the reported protective role of insulin-like growth factor-1, which is able to protect skeletal muscle cells from atrophy via activation of the PI3K–Akt pathway.<sup>45</sup> VEGF, by interacting with VEGFR2, signals through the PI3K–Akt pathway, thus suggesting that VEGF might protect from atrophy by the same pathway. The role of this pathway in muscle atrophy is suggested also by the observation that depletion of TRAF6 in skeletal muscle cells, which is able to induce Akt ubiquitination, preserve muscle fibers from

degradation upon denervation.<sup>46</sup> Further studies are required to address this point.

VEGF treatment, alone or in combination with other anti-atrophic treatments such as physiotherapy, might be particularly useful in case of proximally located nerve lesions owing to the long time required by regenerating axons for reaching the denervated muscles.<sup>47</sup>

On the other hand, as far as improvement of axonal regeneration is concerned, our results showed that VEGF-related anti-atrophic effects on the muscle fiber used as a means for AAV-mediated delivery to regenerating axons made this gene transfer strategy not suitable for this specific application, as reduced muscle atrophy concurrently decreased the number of regenerating axons inside the nerve guide and led to a significant lower functional recovery of the motor function. The failure of the axons regeneration can be explained also with the fact that muscle fibers in the conduit might mimic their original end target (the flexor digitorum sublimis muscle), and therefore be reinnervated by sprouting axons.

Future studies need to go on along two directions. First, alternative means for the delivery of VEGF inside nerve guides should be sought to improve both number and size of regenerating axons. Second, the exploration of alternative molecules to be delivered by AAV-mediated gene transfer inside muscle-vein-combined nerve conduits. In the latter case, it will be important to select genes that code for molecules that do not exert anti-atrophic effect on skeletal muscle fibers.

## MATERIALS AND METHODS

### Experimental design

For this study, we used a total number of 56 adult Wistar rats (weight 250–300 g).

A pilot study was performed in order to evaluate the efficiency of muscle transduction by AAVs. Pectoralis major muscle, then used for the peripheral nerve regeneration study, was injected with AAV2-LacZ or with AAV2-VEGF (four animals per group) and analyzed at the moment of surgery and in the MIV conduits 14 days after surgery. Flexor digitorum sublimis muscle, then used for the study of muscle atrophy, was injected with AAV2-LacZ or with AAV2-VEGF (four animals per group). Injected muscles were analyzed to demonstrate either  $\beta$ -galactosidase or VEGF expression 14 days after injection.

After the preliminary study, the effect of VEGF overexpression on peripheral nerve regeneration was studied in a first experimental group.

The median nerve of adult Wistar rats was cut and repaired with a graft constituted by a vein filled with muscle fibers (MIV) of the pectoralis major previously transduced with either AAV2-VEGF (MIV-VEGF) or AAV2-LacZ (MIV-LacZ, as control; seven animals per group). Functional recovery was assessed by grasping test 3 months after surgery. Regenerated nerves (MIV conduits) were withdrawn 3 months after surgery and analyzed with morphological and stereological techniques.

A second experimental group was used to study the prevention of muscle atrophy evaluating the effect of VEGF overexpression on denervated muscles. The median nerve of adult rats Wistar was transected and the flexor digitorum sublimis muscle was injected with either AAV2-VEGF or AAV2-LacZ (six animals per group). Five rats did not undergo surgery, and the normal flexor digitorum sublimis muscles were withdrawn and used as controls. Transduced muscles were collected 1 month after surgery and analyzed with morphological and stereological techniques.

### Recombinant AAV production

The recombinant AAV vectors used in this study were produced by the AAV Vector Unit at ICGEB Trieste (<http://www.icgeb.org/avu-core-facility.html>), according to the protocol previously described.<sup>12,13,41</sup> All the vectors used in this study express the various complementary DNAs under investigation (hVEGF-A<sub>165</sub>,  $\beta$ -galactosidase) under the control of the constitutive cytomegalovirus immediate early promoter. All the viral stocks used in this study had a titer  $\geq 1 \times 10^{12}$  viral genome particles per ml. The proper expression of all transgenes was tested *in vitro* by western blotting using specific antibodies after transduction of HT1080 cells and *in vivo* by

real-time PCR quantification of the transgene messenger RNAs in transduced tissues.

### Surgical procedure

All animals were housed in a temperature- and humidity-controlled room with 12–12 h light/dark cycles, and were fed with standard chow and water *ad libitum*. Adequate measures were taken to minimize pain and discomfort taking into account human end points for animal suffering and distress. All surgeries were performed with the approval of the local Institution's Animal Care and Ethics Committee and in accordance with the European Communities Council Directive of 24 November 1986 (86/609/EEC). The animals were operated under deep anesthesia by tiletamine-zolazepam (zoletil) intramuscularly (3 mg kg<sup>-1</sup>) with the aid of an operating microscope (Zeiss OPMI 7, Milano, Italy).

**AAV injection.** The muscle, pectoralis major or flexor digitorum sublimis of the forelimb, was exposed and injected with either AAV2-LacZ or AAV2-VEGF (three injections of 20  $\mu$ l corresponding to  $1 \times 10^{11}$  viral genome particles per rat). In the model of peripheral nerve regeneration, the area of injection in the pectoralis major muscle was marked by two suture stitches in order to allow its identification at the moment of the main surgery.

**Median nerve injury and repair.** The median nerve of the left forelimb was approached from the axillary region to the elbow with a longitudinal skin approach and, under operative microscope, was carefully exposed and cut. Transected median nerve was immediately repaired by means of a 10-mm-long graft made by MIV-combined nerve guide. This conduit was constituted by the epigastric vein filled with pectoral muscle fibers transduced by either AAV2-LacZ or AAV2-VEGF.

The muscle fibers of the pectoral muscle were withdrawn and put in the vein longitudinally, so that the basal lamina of myotubes were aligned throughout the length of conduit.<sup>48</sup>

The graft was sutured using three or four stitches of 9–0 monofilament nylon for each stump.<sup>31</sup>

In order to prevent interferences with the grasping test, the contralateral median nerve was transected at the middle third of the brachium and its proximal stump was sutured in the pectoralis major muscle to avoid spontaneous reinnervation.<sup>49</sup>

A 15-mm-long segment of the repaired median nerve (10 mm of graft and 5 mm of distal nerve) was withdrawn 3 months after surgery.

**Muscle denervation.** Flexor digitorum sublimis muscles of the forelimb were denervated by transection of a segment 10-mm-long of the median nerve that, in the rat, is the only nerve controlling these muscles. Both proximal and distal ends of the transected median nerves were twisted and sutured to the fascia superficialis to avoid spontaneous axon regeneration. At the time of surgery, flexor digitorum sublimis muscles were transduced by either AAV2-LacZ or AAV2-VEGF, and harvested 1 month later.

### Biomolecular analysis

Transduced muscles and MIV conduits were harvested and processed for DNA/RNA extraction. In the peripheral nerve regeneration model, at the moment of surgery, the section of injected muscle not used for the conduit preparation was stored for further biomolecular analysis. DNA was extracted using the DNeasy Blood and Tissue kit (Qiagen, Monza, Italy), following manufacturer's instructions. RNA was extracted by TriZol reagent (Invitrogen, Monza, Italy), following manufacturer's instruction, DNase treated and reverse transcribed using random primers. The presence of viral DNA as well as the expression of the transgenes in the tissues were evaluated by real-time PCR using TaqMan probe-based assays (Applied Biosystems, Monza, Italy). The number of viral DNA molecules was calculated on the basis of a standard curve generated from serial dilutions of the pAAV-VEGF plasmid and normalized to DNA amount. For transgene expression, the levels of hVEGF-A and  $\beta$ -galactosidase were normalized by the levels of the housekeeping gene *GAPDH*.

For viral DNA detection, a cytomegalovirus promoter-specific custom PCR assay was used (primer forward 5'-TGGGCGGTAGGCGTGTA-3', primer reverse 5'-CGATCTGACGGTTCCTAAACG-3' and probe FAM (6-carboxy-fluorescein)-TGGGAGGTCTATATAAGC), whereas for transgene expression the following TaqMan predeveloped assays were used: Hs00900055\_m1 (hVEGF-A), Mr03987581\_mr (LacZ) and Rn99999916\_s1 (rat GAPDH). PCR

reactions were performed in a CFX96 Real-Time System (Bio-Rad, Segrate, Milano, Italy).

The complementary DNA was used as a template for real-time PCR amplification to detect the expression levels of pro-apoptotic genes (*Bcl2l11*, *Bmf*, *Bad*); the housekeeping gene *GAPDH* was used to normalize the results. The following predeveloped assays (Applied Biosystems) were used: Rn00674175\_m1 (*Bcl2l11*), Rn00594968\_m1 (*Bmf*) and Rn00575519\_m1 (*Bad*).

### Grasping test

All animals with the median nerve repaired with the MIV were tested with grasping test in order to evaluate the functional recovery 3 months after surgery.

Grasping test was performed following the same procedure previously described,<sup>49</sup> using the BS-GRIP Grip Meter (2Biological Instruments, Varese, Italy). This is a device constituted by a precision balance connected to a grid that the rat can grip. The test is carried out by holding the rat by the tail and putting it close enough to the device to grasp it. The rat is allowed to pull on the bar until it loses the grip. The balance records the maximum weight that the animal manages to hold up before losing the grip. Each animal was tested three times and the average value was recorded.

### Morphology and stereology

The repaired median nerve was removed (10 mm of graft and 5 mm of distal nerve), fixed and prepared for qualitative analysis and quantitative morphometry (stereology) of myelinated nerve fibers. Muscles followed the same procedures.

**Resin embedding.** Nerve and muscle samples were fixed in 2.5% glutaraldehyde, washed in Sorensen phosphate buffer 0.1 M (pH 7.4) with 1.5% saccharose and post-fixed in 2% osmium tetroxide for 2 h. After dehydration in ethanol, samples were cleared in propylene oxide and embedded in Glauert's embedding mixture of resins consisting in equal parts of Araldite M and Araldite Harter, HY 964 (Merck, Darmstadt, Germany), containing 0.5% of the plasticizer dibutyl phthalate and 1–2% of the accelerator 964, DY 064 (Merck).

**Light microscopy and stereology.** For high-resolution light microscopy, 2.5  $\mu$ m transversal cross-sections of the repaired median nerve and muscle samples were obtained using an Ultracut UCT ultramicrotome (Leica Microsystems, Wetzlar, Germany). Sections were stained by toluidine blue and used for qualitative and quantitative morphological analysis that was performed using a DM4000B microscope equipped with a DFC320 digital camera and an IM50 image manager system (Leica Microsystems).

One semithin section from each nerve and from each muscle was randomly selected and used for the quantitative analysis.

The total cross-sectional area of the nerve was measured and sampling fields were then randomly selected using a protocol previously described.<sup>50,51</sup> Bias arising from the 'edge effect' was coped with the employment of a two-dimensional disector procedure that is based on sampling the 'tops' of fibers.<sup>52,53</sup> Mean fiber density in each disector was then calculated by dividing the number of nerve fibers counted by the disector's area ( $N \text{ mm}^{-2}$ ). Finally, total fiber number ( $N$ ) in the nerve was estimated by multiplying the mean fiber density by the total cross-sectional area of the whole nerve. Two-dimensional disector probes were also used for the unbiased selection of a representative sample of myelinated nerve fibers for estimating circle-fitting diameter and myelin thickness.

The same stereological principles were used for muscle fibers' cross-sectional area estimation.

**Electron microscopy.** For electron microscopy, transversal cross-sections of 70 nm were obtained from the middle part of the muscle-vein-combined graft, using an Ultracut UCT ultramicrotome (Leica Microsystems).

Sections were then stained with uranyl acetate and lead citrate, and examined by a JEM-1010 transmission electron microscope (JEOL, Tokyo, Japan) equipped with a Mega-View-III digital camera and a Soft-Imaging-System (SIS, Münster, Germany) for the computerized acquisition of the images.

**Immunofluorescence.** For immunofluorescence, tissue were harvested 30 days after main surgery and snap-frozen in liquid nitrogen-cooled isopentane. Frozen sections (5  $\mu$ m thick) were stained using the following primary antibodies: anti-slow myosin heavy chain (clone NOQ7.5AD,

Sigma) and anti-laminin (Sigma, Milano, Italy); Alexa488 conjugated goat anti-rabbit and Alexa594 conjugated donkey anti-mouse (both from Molecular Probes, Monza, Italy) were used as secondary antibodies.

Images were acquired with a DMLC upright fluorescence microscope (Leica Microsystems, Milano, Italy) equipped with a charge-coupled device camera (CoolSNAP CF, Roper Scientific, Roma, Italy) using MetaView 4.6 quantitative analysis software (MDS Analytical Technologies, Sunnyvale, CA, USA). Relative areas occupied by differently stained cells were quantified by the use of ImageJ software (National Institutes of Health, Bethesda, MD, USA).

### Statistical analysis

Results obtained were averaged and expressed as means  $\pm$  s.e.m. Analysis of variance and Student–Newman–Keuls tests were used to compare data from different groups.

### CONFLICT OF INTEREST

The authors declare no conflict of interest.

### ACKNOWLEDGEMENTS

This research was supported by the Compagnia di San Paolo (MOVAG project), the Regione Piemonte (Ricerca Sanitaria Finalizzata) and the European Community's Seventh Framework Programme (FP7-HEALTH-2011) under Grant agreement number 278612.

### REFERENCES

- Homs J, Ariza L, Pages G, Udina E, Navarro X, Chillon M *et al*. Schwann cell targeting via intrasciatic injection of AAV8 as gene therapy strategy for peripheral nerve regeneration. *Gene Therapy* 2011; **18**: 622–630.
- Ortolano S, Spuch C, Navarro C. Present and future of adeno associated virus based gene therapy approaches. *Recent Pat Endocr Metab Immune Drug Discov* 2012; **6**: 47–66.
- Geuna S, Raimondo S, Ronchi G, Di Scipio F, Tos P, Czaja K *et al*. Chapter 3: Histology of the peripheral nerve and changes occurring during nerve regeneration. *Int Rev Neurobiol* 2009; **87**: 27–46.
- Ahad MA, Fogerson PM, Rosen GD, Narayanaswami P, Rutkove SB. Electrical characteristics of rat skeletal muscle in immaturity, adulthood and after sciatic nerve injury, and their relation to muscle fiber size. *Physiol Meas* 2009; **30**: 1415–1427.
- Isaacs J, Loveland K, Mallu S, Adams S, Wodicka R. The use of anabolic steroids as a strategy in reversing denervation atrophy after delayed nerve repair. *Hand (N Y)* 2011; **6**: 142–148.
- Aydin MA, Mackinnon SE, Gu XM, Kobayashi J, Kuzon Jr. WM. Force deficits in skeletal muscle after delayed reinnervation. *Plast Reconstr Surg* 2004; **113**: 1712–1718.
- Kobayashi J, Mackinnon SE, Watanabe O, Ball DJ, Gu XM, Hunter DA *et al*. The effect of duration of muscle denervation on functional recovery in the rat model. *Muscle Nerve* 1997; **20**: 858–866.
- Carlson B, Borisov AB, Dedkov EI, Dow D, Kostrominova T. The Biology and Restorative Capacity of Long-Term Denervated Skeletal Muscle. *Basic Appl Myol* 2002; **12**: 247–254.
- Karvinen H, Pasanen E, Rissanen TT, Korpisalo P, Vahakangas E, Jazwa A *et al*. Long-term VEGF-A expression promotes aberrant angiogenesis and fibrosis in skeletal muscle. *Gene Therapy* 2011; **18**: 1166–1172.
- Abadie J, Blouin V, Guigand L, Wyers M, Chereh Y. Recombinant adeno-associated virus type 2 mediates highly efficient gene transfer in regenerating rat skeletal muscle. *Gene Therapy* 2002; **9**: 1037–1043.
- Messina S, Mazzeo A, Bitto A, Aguenouz M, Migliorato A, De Pasquale MG *et al*. VEGF overexpression via adeno-associated virus gene transfer promotes skeletal muscle regeneration and enhances muscle function in mdx mice. *FASEB J* 2007; **21**: 3737–3746.
- Arsic N, Zentilin L, Zacchigna S, Santoro D, Stanta G, Salvi A *et al*. Induction of functional neovascularization by combined VEGF and angiotensin-1 gene transfer using AAV vectors. *Mol Ther* 2003; **7**: 450–459.
- Arsic N, Zacchigna S, Zentilin L, Ramirez-Correa G, Patarini L, Salvi A *et al*. Vascular endothelial growth factor stimulates skeletal muscle regeneration *in vivo*. *Mol Ther* 2004; **10**: 844–854.
- Deumens R, Bozkurt A, Meek MF, Marcus MA, Joosten EA, Weis J *et al*. Repairing injured peripheral nerves: bridging the gap. *Prog Neurobiol* 2010; **92**: 245–276.
- Giacca M, Zacchigna S. VEGF gene therapy: therapeutic angiogenesis in the clinic and beyond. *Gene Therapy* 2012; **19**: 622–629.

- 16 Haninec P, Kaiser R, Bobek V, Dubovy P. Enhancement of musculocutaneous nerve reinnervation after vascular endothelial growth factor (VEGF) gene therapy. *BMC Neurosci* 2012; **13**: 57.
- 17 Sondell M, Lundborg G, Kanje M. Vascular endothelial growth factor stimulates Schwann cell invasion and neovascularization of acellular nerve grafts. *Brain Res* 1999; **846**: 219–228.
- 18 Frey SP, Jansen H, Raschke MJ, Meffert RH, Ochman S. VEGF improves skeletal muscle regeneration after acute trauma and reconstruction of the limb in a rabbit model. *Clin Orthop Relat Res* 2012; **470**: 3607–3614.
- 19 Rosenstein JM, Krum JM, Ruhrberg C. VEGF in the nervous system. *Organogenesis* 2010; **6**: 107–114.
- 20 Rissanen TT, Vajanto I, Hiltunen MO, Rutanen J, Kettunen MI, Niemi M *et al*. Expression of vascular endothelial growth factor and vascular endothelial growth factor receptor-2 (KDR/Flk-1) in ischemic skeletal muscle and its regeneration. *Am J Pathol* 2002; **160**: 1393–1403.
- 21 Tos P, Ronchi G, Papalia I, Sallen V, Legagneux J, Geuna S *et al*. Chapter 4: Methods and protocols in peripheral nerve regeneration experimental research: part I-experimental models. *Int Rev Neurobiol* 2009; **87**: 47–79.
- 22 Tafuro S, Ayuso E, Zacchigna S, Zentilin L, Moimas S, Dore F *et al*. Inducible adeno-associated virus vectors promote functional angiogenesis in adult organisms via regulated vascular endothelial growth factor expression. *Cardiovasc Res* 2009; **83**: 663–671.
- 23 Borselli C, Storrie H, Benesch-Lee F, Shvartsman D, Cezar C, Lichtman JW *et al*. Functional muscle regeneration with combined delivery of angiogenesis and myogenesis factors. *Proc Natl Acad Sci USA* 2010; **107**: 3287–3292.
- 24 Yegiyants S, Dayicioglu D, Kardashian G, Panthaki ZJ. Traumatic peripheral nerve injury: a wartime review. *J Craniofac Surg* 2010; **21**: 998–1001.
- 25 Siemionow M, Bozkurt M, Zor F. Regeneration and repair of peripheral nerves with different biomaterials: review. *Microsurgery* 2010; **30**: 574–588.
- 26 Gu X, Ding F, Yang Y, Liu J. Construction of tissue engineered nerve grafts and their application in peripheral nerve regeneration. *Prog Neurobiol* 2010; **93**: 204–230.
- 27 Zachary I. Neuroprotective role of vascular endothelial growth factor: signalling mechanisms, biological function, and therapeutic potential. *Neurosignals* 2005; **14**: 207–221.
- 28 Eppler SM, Combs DL, Henry TD, Lopez JJ, Ellis SG, Yi JH *et al*. A target-mediated model to describe the pharmacokinetics and hemodynamic effects of recombinant human vascular endothelial growth factor in humans. *Clin Pharmacol Ther* 2002; **72**: 20–32.
- 29 Giacca M. Virus-mediated gene transfer to induce therapeutic angiogenesis: where do we stand? *Int J Nanomed* 2007; **2**: 527–540.
- 30 Riviere C, Danos O, Douar AM. Long-term expression and repeated administration of AAV type 1, 2 and 5 vectors in skeletal muscle of immunocompetent adult mice. *Gene Therapy* 2006; **13**: 1300–1308.
- 31 Geuna S, Tos P, Battiston B, Giacobini-Robecchi MG. Bridging peripheral nerve defects with muscle-vein combined guides. *Neuro Res* 2004; **26**: 139–144.
- 32 Battiston B, Raimondo S, Tos P, Gaidano V, Audisio C, Scevola A *et al*. Chapter 11: Tissue engineering of peripheral nerves. *Int Rev Neurobiol* 2009; **87**: 227–249.
- 33 Manno CS, Chew AJ, Hutchison S, Larson PJ, Herzog RW, Arruda VR *et al*. AAV-mediated factor IX gene transfer to skeletal muscle in patients with severe hemophilia B. *Blood* 2003; **101**: 2963–2972.
- 34 Buchlis G, Podsakoff GM, Radu A, Hawk SM, Flake AW, Mingozzi F *et al*. Factor IX expression in skeletal muscle of a severe hemophilia B patient 10 years after AAV-mediated gene transfer. *Blood* 2012; **119**: 3038–3041.
- 35 Kay MA, Manno CS, Ragni MV, Larson PJ, Couto LB, McClelland A *et al*. Evidence for gene transfer and expression of factor IX in haemophilia B patients treated with an AAV vector. *Nat Genet* 2000; **24**: 257–261.
- 36 Buning H, Nicklin SA, Perabo L, Hallek M, Baker AH. AAV-based gene transfer. *Curr Opin Mol Ther* 2003; **5**: 367–375.
- 37 Giacca M. *Gene Therapy*. 1st edn, vol. 306. Springer: New York, USA, 2010, p 80.
- 38 Wu Z, Asokan A, Samulski RJ. Adeno-associated virus serotypes: vector toolkit for human gene therapy. *Mol Ther* 2006; **14**: 316–327.
- 39 Zentilin L, Giacca M. Adeno-associated virus vectors: versatile tools for *in vivo* gene transfer. *Contrib Nephrol* 2008; **159**: 63–77.
- 40 Macedo A, Moriggi M, Vasso M, De Palma S, Sturnega M, Friso G *et al*. Enhanced athletic performance on multisite AAV-IGF1 gene transfer coincides with massive modification of the muscle proteome. *Hum Gene Ther* 2012; **23**: 146–157.
- 41 Zacchigna S, Pattarini L, Zentilin L, Moimas S, Carrer A, Sinigaglia M *et al*. Bone marrow cells recruited through the neuropilin-1 receptor promote arterial formation at the sites of adult neoangiogenesis in mice. *J Clin Invest* 2008; **118**: 2062–2075.
- 42 Guzzini M, Raffa S, Geuna S, Nicolino S, Torrisi MR, Tos P *et al*. Denervation-related changes in acetylcholine receptor density and distribution in the rat flexor digitorum sublimis muscle. *Ital J Anat Embryol* 2008; **113**: 209–216.
- 43 Rahimi N. The ubiquitin-proteasome system meets angiogenesis. *Mol Cancer Ther* 2012; **11**: 538–548.
- 44 McKinnell IW, Rudnicki MA. Molecular mechanisms of muscle atrophy. *Cell* 2004; **119**: 907–910.
- 45 Bodine SC, Stitt TN, Gonzalez M, Kline WO, Stover GL, Bauerlein R *et al*. Akt/mTOR pathway is a crucial regulator of skeletal muscle hypertrophy and can prevent muscle atrophy *in vivo*. *Nat Cell Biol* 2001; **3**: 1014–1019.
- 46 Paul PK, Gupta SK, Bhatnagar S, Panguluri SK, Darnay BG, Choi Y *et al*. Targeted ablation of TRAF6 inhibits skeletal muscle wasting in mice. *J Cell Biol* 2010; **191**: 1395–1411.
- 47 Fu SY, Gordon T. Contributing factors to poor functional recovery after delayed nerve repair: prolonged denervation. *J Neurosci* 1995; **15**: 3886–3895.
- 48 Raimondo S, Nicolino S, Tos P, Battiston B, Giacobini-Robecchi MG, Perroteau I *et al*. Schwann cell behavior after nerve repair by means of tissue-engineered muscle-vein combined guides. *J Comp Neurol* 2005; **489**: 249–259.
- 49 Papalia I, Tos P, Stagno d'Alcontres F, Battiston B, Geuna S. On the use of the grasping test in the rat median nerve model: a re-appraisal of its efficacy for quantitative assessment of motor function recovery. *J Neurosci Methods* 2003; **127**: 43–47.
- 50 Geuna S, Tos P, Battiston B, Guglielmo R. Verification of the two-dimensional disector, a method for the unbiased estimation of density and number of myelinated nerve fibers in peripheral nerves. *Ann Anat* 2000; **182**: 23–34.
- 51 Larsen JO. Stereology of nerve cross sections. *J Neurosci Methods* 1998; **85**: 107–118.
- 52 Schmitz C. Variation of fractionator estimates and its prediction. *Anat Embryol (Berl)* 1998; **198**: 371–397.
- 53 Geuna S. Appreciating the difference between design-based and model-based sampling strategies in quantitative morphology of the nervous system. *J Comp Neurol* 2000; **427**: 333–339.



This work is licensed under a Creative Commons Attribution-NonCommercial-NoDerivs 3.0 Unported License. To view a copy of this license, visit <http://creativecommons.org/licenses/by-nc-nd/3.0/>

Supplementary Information accompanies this paper on Gene Therapy website (<http://www.nature.com/gt>)